

# Physical Properties of Polyethylene/Silicate Nanocomposite Blown Films

Ki Hyun Wang, Chong Min Koo, In Jae Chung

Department of Chemical and Biomolecular Engineering, KAIST, 373-1, Guseong-dong, Yuseong-gu, Daejeon 305-701, South Korea

Received 28 May 2002; accepted 17 September 2002

**ABSTRACT:** Maleated polyethylene/silicate nanocomposite and maleated polyethylene/SiO<sub>2</sub> blown films were prepared by melt extrusion. The silicate and SiO<sub>2</sub> significantly affected the physical properties of the films. The former films showed higher tensile strength than the latter films. This high reinforcement effect seemed to be attributable to the strong interaction between the matrix and silicate as well as the uniform dispersion of silicate layers in the polymer matrix. The addition of silicate beyond a certain content gave a worse Elmendorf tear strength than SiO<sub>2</sub>. The silicate did not increase the falling dart impact strength at

all. The worst Elmendorf strength apparently originated from the orientation of anisotropic silicate rather than the orientation of lamellae of the polymer matrix, and the silicate made the films more brittle. The well-dispersed silicate layers in the polymer matrix gave almost the same optical properties as the pure polymer despite the increase in the silicate content. © 2003 Wiley Periodicals, Inc. *J Appl Polym Sci* 89: 2131–2136, 2003

**Key words:** polyethylene (PE); nanocomposites; films

## INTRODUCTION

It is well established that the effective dispersion of anisotropic particles with high aspect ratios, such as short fibers, plates, and whiskers, within a continuous polymer matrix, in combination with adequate interfacial adhesion between the filler and polymer, can account for substantially improved reinforcement of the polymer matrix.<sup>1</sup> Layered-silicate-based polymer nanocomposites have attracted considerable technological and scientific interest in recent years<sup>2–5</sup> because they have shown dramatic enhancements in the physical, thermal, and mechanical properties of polymers even with a very low loading of silicate.<sup>5</sup> Pioneering advances at Toyota during the early 1990s stimulated the development of various polymer/organosilicate nanocomposites with attractive improved property profiles.<sup>6</sup>

In thermoplastic-based (intercalated or exfoliated) nanocomposites, the ultimate strength that the material can bear before the break may vary strongly, depending on the nature of the interactions between the matrix and filler. As far as polypropylene (PP)-based nanocomposites are concerned,<sup>7</sup> very slight tensile stress enhancements are measured. This behavior can partially be explained by the lack of interfacial adhesion between apolar PP and polar layered silicates.

The addition of PP modified with maleic anhydride (MA) to the PP matrix has, however, proven to be favorable to the intercalation of the PP chains and maintains the ultimate stress at an acceptable level.

Polyethylene is one of the most widely used polyolefin polymers. Because it does not include any polar group in its backbone like PP, it is thought that the homogeneous dispersion of the hydrophilic silicate layers in polyethylene is not realized. In our previous report, we noted that polyethylene grafted with MA could exfoliate organically modified silicate layers.<sup>8</sup> The dispersion mechanism is highly dependent on the hydrophilicity of the polyethylene grafted with MA and the hydrophobicity of the organically modified silicate.

Most polyethylene is used in film applications. Polyethylene films for packaging applications are commonly made with a blown-film process.<sup>9</sup> Some examples of packaging applications include food packaging, trashcan liners, shrink films, stretch films, and merchandise packaging. Packaging films are required to possess high clarity and high strength in most applications. With such blown-film properties, even though the incorporation of some fillers enhances the strength of the film, it has a worse effect on the film clarity.

In this article, we report the mechanical and optical properties of nanocomposite blown films. To achieve a fundamental understanding of silicate or common filler reinforcements, we compare the properties of films made from different fillers, silicate and SiO<sub>2</sub>.

Correspondence to: I. J. Chung (chung@kaist.ac.kr).

## EXPERIMENTAL

### Materials

The materials used for the synthesis of the nanocomposites were modified montmorillonite (Cloisite 20A) from Southern Clay Products and polyethylene modified with maleic anhydride (PEMA). The modified silicate (20A; density = 1.75 g/cc) was ion-exchanged with dimethyl dihydrogenated tallow ammonium ions (the tallow was composed predominantly of octadecyl chains with smaller amounts of lower homologues; the approximate composition was 65% C<sub>18</sub>, 30% C<sub>16</sub>, and 5% C<sub>14</sub>). We prepared PEMA by melt blending maleated polyethylene from Aldrich and pure linear low-density polyethylene (LLDPE; Han Wha Chemical Corp.) in a twin-screw extruder (Gottfert Corp.; screw diameter = 19 mm) at a constant rotating speed of 30 rpm. The maleated polyethylene from Aldrich was LLDPE (density = 0.930 g/cc) grafted with 0.85 wt % MA, and it had a weight-average molecular weight of 126,000 according to gel permeation chromatography (GPC). The pure LLDPE had a melt index of 1.0, a density of 0.920 g/cc, and a weight-average molecular weight of 180,000 according to GPC. As a conventional filler, SiO<sub>2</sub> (density = 2.59 g/cc, average particle size = 1.8 μm) was purchased from Fuji Sylysia. The density of the materials was measured with a pycnometer (AccuPyc 1330, Micromeritics).

For measuring the content of MA grafted onto LLDPE, the samples obtained after melt blending were dissolved in xylene at a concentration of 2 wt %. This solution was mixed with acetone, and the precipitate was filtered and dried again in a vacuum oven at 60°C for 24 h. The percentage of MA grafted onto LLDPE was determined by elemental analysis.<sup>9</sup>

### Preparation of the composites and films

We prepared resins for nanocomposite and conventional composite films with a twin extruder. These resins for films were made from the melt blending of PEMA, LLDPE, and a proper amount of silicate or SiO<sub>2</sub> in a twin-screw extruder (Gottfert Corp.; screw diameter = 19 mm) at a constant rotating speed of 30 rpm and with a barrel (length/diameter = 25) temperature profile of 150–200°C. These mixtures were premixed in a Henschel mixer before they were fed into the twin extruder.

The films were prepared with tubular blown LLDPE film equipment at a 2.0 blowup ratio. The equipment had a screw with a 40-mm diameter, a length/diameter ratio of 24, and a 75-mm spiral die with a die gap of 2 mm. The film thickness was controlled to be 30 μm. The processing temperature was kept at 170–190°C, and the flow rate was 12 kg/h.

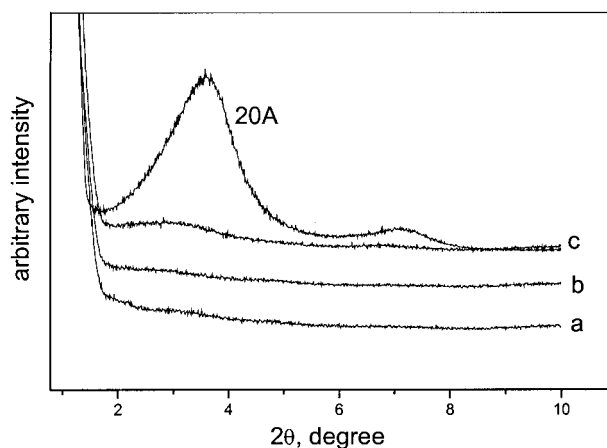


**Figure 1** XRD patterns of the PEMA/20A films and pure silicate (20A): (a) 0.5, (b) 1.0, and (c) 1.5 vol % 20A.

### Measurements

X-ray diffraction (XRD) was used to observe the dispersability of the silicate in composites. XRD measurements were carried out on a Rigaku X-ray generator (Cu K $\alpha$  radiation with  $\lambda = 0.15406$  nm) at room temperature. The diffractograms were scanned in a  $2\theta$  range of 1.2–10° at a rate of 2°/min.

The mechanical tensile properties of the films were measured according to ASTM D 882 with an Instron 4204. The crosshead speed was 500 mm/min. The dart drop impact resistance was measured according to ASTM D 1709 (method A). The Elmendorf tear strength was determined according to ASTM D 1922. The X-ray two-dimensional patterns were obtained with a Siemens GADDS (general area detection diffraction system) two-dimensional detector. The distance from the sample to the detector was 120 mm. The haze for optical properties was determined according to ASTM D 1003.

## RESULTS AND DISCUSSION

### Preparation of the nanocomposite films by blowing extrusion

The MA grafting level of polyethylene is important to the morphology of polyethylene/silicate nanocomposites. We prepared PEMA by the melt blending of 85 wt % pure LLDPE with 15 wt % maleated polyethylene. The grafted levels of MA in PEMA, as measured by elemental analysis, were 0.12 wt %.<sup>8</sup> The 20A and SiO<sub>2</sub> contents in the films were controlled to be 0.5, 1.0, and 1.5 vol %. The films with 20A and SiO<sub>2</sub> were denoted PEMA/20A and PEMA/SiO<sub>2</sub>, respectively.

Figure 1 portrays the XRD patterns of the blown films with 20A. The original basal reflection peak of 20A in films with 0.5 and 1.0 vol % 20A disappeared. This fact reveals that the silicates were exfoliated and well dispersed in the film matrix. However, in the film

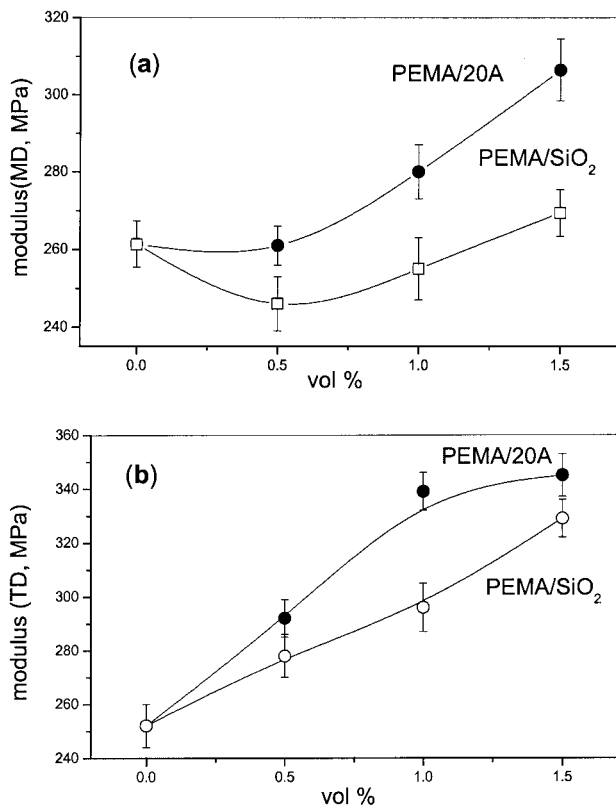


Figure 2 Young's modulus of the films at a 500 mm/min extension rate: (a) MD and (b) TD.

with 1.5 vol % 20A, a weak peak was found at a lower angle than for silicate 20A. This indicates that the silicates were partly intercalated by PEMA, but most of them were well dispersed in the film matrix.<sup>8</sup>

**Tensile properties of the films**

The effects of the contents of 20A and SiO<sub>2</sub> on the tensile properties of the films were investigated. Figure 2 shows Young's modulus in the machine direction (MD) and transverse direction (TD) for the films. The modulus in both the MD and TD increased rapidly with the 20A contents increasing from 0.5 to 1.5 vol %. The PEMA/SiO<sub>2</sub> films increased less than the films with 20A. This means that the addition of the silicate filler increased the stiffness of the films more. The tensile strength at break of the films is shown in Figure 3. Just as for the modulus, the PEMA/20A films depicted increased tensile strength at break in the MD [Fig. 3(a)], but the strength was constant in the TD up to 1 vol %, and decreased strength was displayed beyond the higher concentration of 20A [Fig. 3(b)]. It seems that the addition of silicate beyond a certain content could not increase the tensile strength of PEMA/20A more. It is relevant to the orientation of the silicate layers, not the intercalated state. This is discussed later. PEMA/SiO<sub>2</sub> films had a lower

strength at break than pure PEMA and PEMA/20A films at the same filler contents. Besides, PEMA/20A films displayed a higher elongation at break than PEMA/SiO<sub>2</sub> films at all filler contents, as shown in Figure 4. Because the inorganic filler particles were rigid, they could not be deformed by external stress in the specimens but acted only as stress concentrators during deformation processes. PEMA/SiO<sub>2</sub> had a steeper decrease in the elongation at break than PEMA/20A. This sharp decrease suggests that the SiO<sub>2</sub> particles had weak interactions with PEMA because they were dispersed poorly and were large. On the basis of these results, it can be summarized that the nanocomposite films could attain superior performance over their counterpart conventional films because of the strong interactions between the matrix and silicate, the nanoscale size of silicate, and the uniform dispersion of silicate layers in the PEMA matrix.

**Tear properties of the films**

The Elmendorf tear test is a measure of resistance to the propagation of a tear, which is initiated with a preintroduced slit in a specimen. Figure 5 provides the Elmendorf tear strength of the films. For all of the films, the Elmendorf strength in the TD exceeds that in

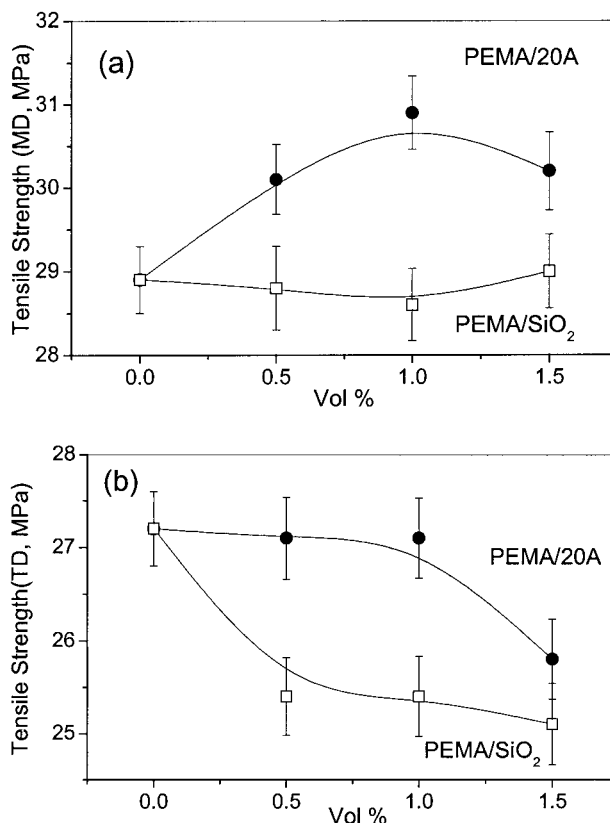
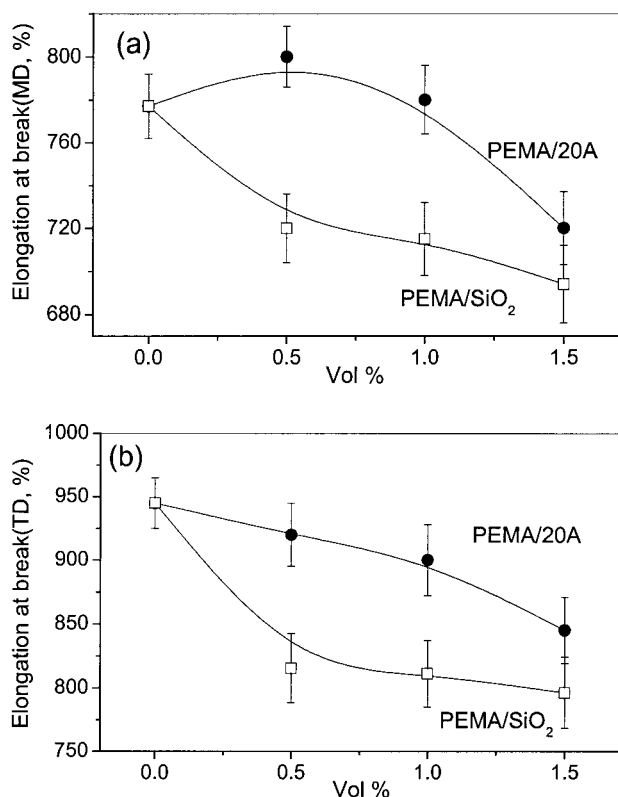


Figure 3 Tensile strength at break of the films with the filler contents: (a) MD and (b) TD.



**Figure 4** Elongation at break of the films with the filler contents: (a) MD and (b) TD.

the MD. The Elmendorf tear behavior was highly influenced by the orientation distribution of the lamellar stacks with respect to the tearing direction. The preferential orientation of the lamellar stacks parallel to the MD was responsible for the low tear strength in the MD and the imbalance between the MD and TD tear strengths of the blown films. As the polymer molecules exited the film die, the extensional forces applied tended to orient them along the stresses. The relaxation of the extended conformation of these polymer chains simultaneously competed with their orientation before the crystallization process. Consequently, at high MD extension rates, a greater number of molecules were oriented along the MD before the onset of crystallization. When a film was blown at a low MD extension rate, it tended to offer greater resistance to tear propagation along the MD.<sup>11</sup> Figure 5 shows that the PEMA/20A films had higher TD tear strengths than PEMA/SiO<sub>2</sub> at all filler contents. However, the former gave a lower MD strength than the latter at 1.5 vol % filler contents. It seems that the silicate might have given a more oriented pattern of blown films than general fillers when the filler contents reached beyond certain contents.

In this study, all the films were prepared under the same processing conditions, including the blowup ratio and extrusion rate. Figure 6 portrays three diffraction patterns for films with 1.5 vol % fillers in three

directions: through, edge, and end. Through is the direction normal to the film surface. The edge and end directions are parallel to the film thickness direction and film rolling direction, respectively. In the through patterns, the reflections (Debye-Scherrer rings) from the (110) and (200) crystal planes are evident. The intensity of the (200) reflection is concentrated along the meridian plane for all three films. Furthermore, the intensity of the (110) reflection has a maximum away from the equatorial plane. These observations indicate preferential orientation of the *a* axis along the film MD in these films. The through pattern of PEMA/20A did not show any reflection near the beam stopper like other films. However, in the edge and end patterns of PEMA/20A, strong and anisotropic intensity peaks, which correspond to the (001) reflection of montmorillonite<sup>12,13</sup>, can be seen on the equator near the beam stopper. This reflects the strong orientation of silicate.<sup>14</sup>

From these results, it seems that the decreasing Elmendorf tear strength of PEMA/20A films in the MD beyond certain contents of 20A originated from the orientation of anisotropic silicate to the MD rather than the orientation of lamellae of PEMA.

The dart drop impact strength of all the films is given in Figure 7. The dart drop impact strength of the

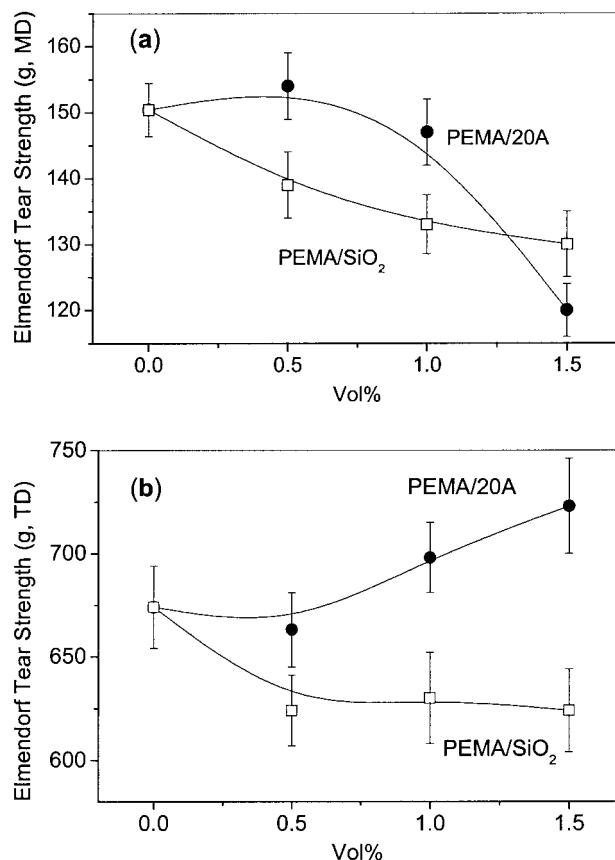


**Figure 5** Elmendorf tear strength of the films with the filler contents: (a) MD and (b) TD.

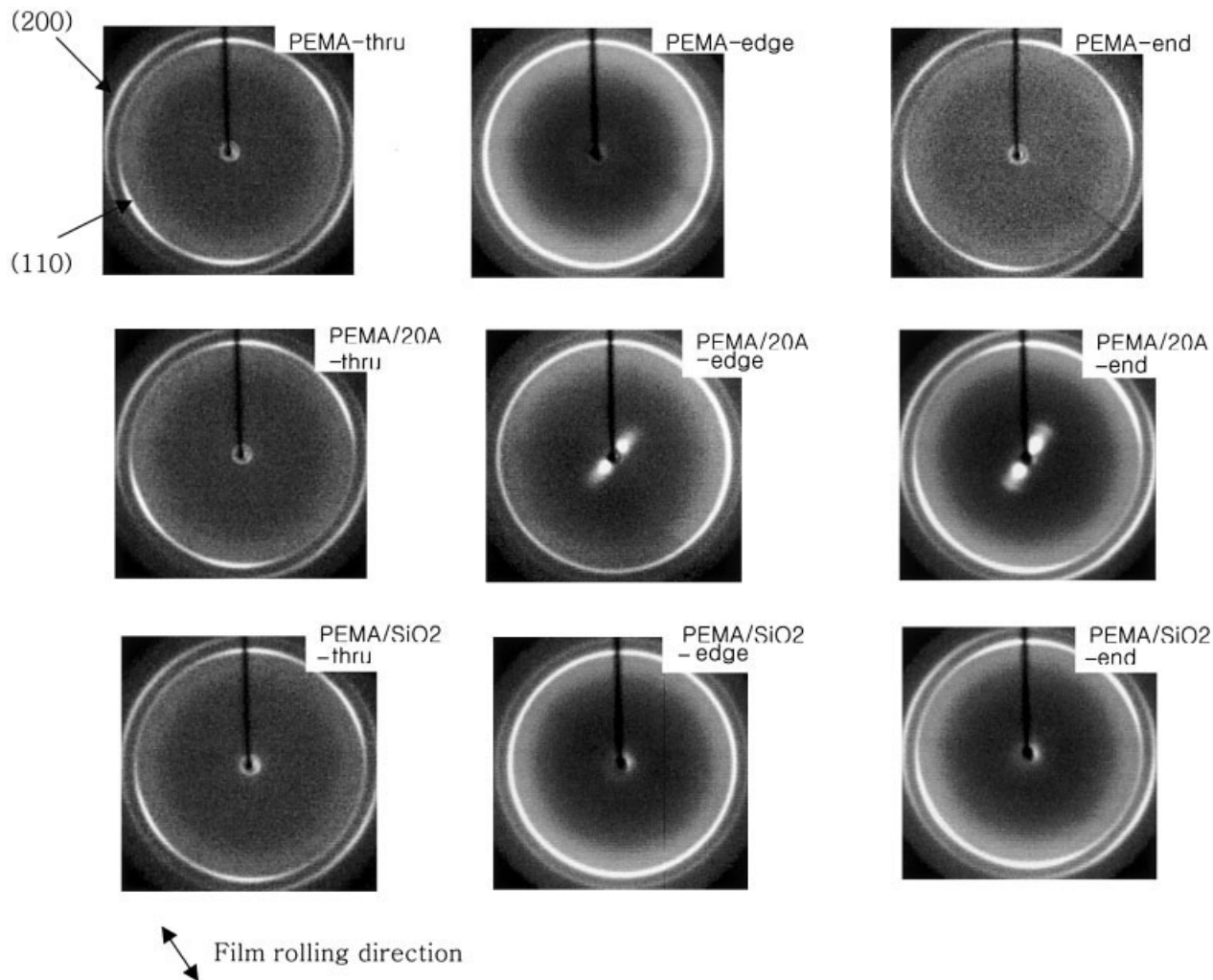


Figure 6 XRD patterns of the films with 1.5 vol % filler contents.

films significantly depended on the overall blowing conditions, including the blowup ratio and MD extension rate. The imbalance of orientation between the MD and TD was responsible for the low dart impact strength. Even though the PEMA/20A films showed

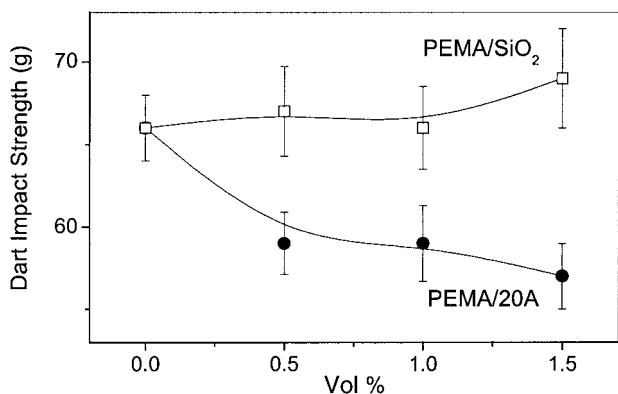
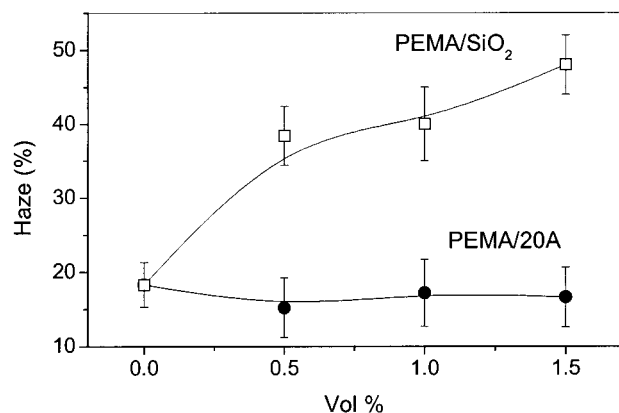


Figure 7 Dart impact strength of the films with the filler contents.

better Elmendorf strength and elongation at break in both the MD and TD than PEMA/SiO<sub>2</sub> until 1 vol % filler, they had worse properties than PEMA/SiO<sub>2</sub> films. It seems that the silicate improved the stiffness of the films more than SiO<sub>2</sub>, but it did not increase the instant impact strength, including the falling dart strength. In other words, PEMA/20A was more brittle than PEMA/SiO<sub>2</sub>, like a solid. In our previous reports,<sup>14,15</sup> nanocomposite with high aspect ratios of silicate showed a solidlike rheological behavior beyond certain contents in the matrix.

**Optical properties of the films**

Figure 8 displays the haze properties of all the films. It is evident that departures from perfect transparency were due to light scattering by the samples, which degraded the information carried by the directly transmitted beam. The forward scattered flux may be subdivided into two ranges of scattering angles: from 0 to 5° and from 5 to 90°. Haze is defined as the



**Figure 8** Haze variation of the films with the filler contents.

fraction of the transmitted light that deviates from the directly transmitted beam by more than  $5^\circ$ .<sup>16</sup> PEMA/SiO<sub>2</sub> had a monotonic increase in the haze value with an increasing loading of SiO<sub>2</sub>. On the contrary, silicate gave almost the same value despite the increasing content of silicate. It is believed that the 20A inclusion did not adversely influence the LLDPE film optics because of its dispersion on the order of the wavelength of visible light. However, the general filler, SiO<sub>2</sub>, greatly influenced the optics because of its dispersion over the order of the wavelength of visible light.

### CONCLUSIONS

Nanocomposite PEMA/20A blown films revealed the exfoliated state and intercalated state according to the content of silicate. The film properties of PEMA/20A and PEMA/SiO<sub>2</sub> were compared. PEMA/20A showed higher modulus, tensile strength, and elongation properties than PEMA/SiO<sub>2</sub>. This high strength seems to be due to the strong interaction between the matrix and silicate and the nanoscale size of silicate, as well as the uniform dispersion of silicate layers in the PEMA matrix.

PEMA/20A gave a higher TD Elmendorf tear strength but a lower MD strength at 1.5 vol % filler contents than PEMA/SiO<sub>2</sub>. This was caused by the orientation of anisotropic silicate to the MD rather than the orientation of lamellae of PEMA. As for the dart impact strength, the PEMA/20A films showed worse properties than PEMA/SiO<sub>2</sub> films. It seems that silicate led to more brittle properties than SiO<sub>2</sub>. Silicate did not hurt the optical properties despite an increasing content of silicate, whereas the SiO<sub>2</sub> filler led to worse optical properties with the filler contents. This indicates that silicate was well dispersed at the molecular level in the film matrix.

### References

1. Handbook of Fillers for Plastics; Katz, H. S.; Milewski, J. V., Eds.; Van Nostrand Reinhold: New York, 1987.
2. Giannelis, E. P. *Adv Mater* 1996, 8, 29.
3. Giannelis, E. P.; Krishnamoorti, R.; Manias, E. *Adv Polym Sci* 1995, 33, 1047.
4. Krishnamoorti, E.; Vaia, R. A.; Giannelis, E. P. *Chem Mater* 1996, 8, 1718.
5. Kojima, Y.; Usuki, A.; Kawasumi, M.; Okada, A.; Fukushima, Y.; Kurauchi, T.; Kamigaito, O. *J Mater Res* 1993, 8, 1185.
6. Okada, A.; Kojima, Y.; Kawasumi, M.; Fukushima, Y.; Kuranchi, T.; Kamigaito, O. *J Mater Res* 1993, 8, 1179.
7. Hasegawa, N.; Kawasumi, M.; Kato, M.; Usuki, A.; Okada, A. *J Appl Polym Sci* 1998, 67, 87.
8. Wang, K. H.; Choi, M. H.; Koo, C. M.; Choi, Y. S.; Chung, I. J. *Polymer* 2001, 42, 9819.
9. White, J. L.; Cakmak, M. I.; Mark, H. F.; Kikales, N.; Overberger, C.; Menges, G. *Encyclopedia of Polymer Science and Engineering*; Wiley-Interscience: New York, 1987; Vol. 10, p 619.
10. Rong, M. Z.; Zhang, M. Q.; Zheng, Y. X.; Zeng, H. M.; Water, R. *Polymer* 2001, 42, 167.
11. Krishnaswamy, R. K.; Sukhadia, A. M. *Polymer* 2001, 41, 9205.
12. Fukushima, Y. *Clays Clay Miner* 1984, 32, 320.
13. Ogata, N.; Kawakage, S.; Ogihara, T. *Polymer* 1997, 38, 5115.
14. Wang, K. H.; Xu, M.; Choi, Y. S.; Chung, I. J. *Polym Bull* 2001, 46, 499.
15. Wang, K. H.; Choi, M. H.; Koo, C. M.; Xu, M.; Chung, I. J.; Jang, M. C.; Choi, S. W.; Song, H. H. *J Polym Sci Part B: Polym Phys* 2002, 40, 1454.
16. Meeten, G. H. *Optical Properties of Polymers*; Elsevier Applied Science: London, 1986; p 277.